

# Multibody dynamics approaches of the humerus-shoulder complex driven by multimuscle activations and constraints

T. Tsuta<sup>1</sup>, Y. Takeda<sup>2</sup> & T. Iwamoto<sup>2</sup>

<sup>1</sup>*Hiroshima International University, Japan*

<sup>2</sup>*Graduate School of Hiroshima University, Japan*

## Abstract

A multibody dynamics approach of the humerus-shoulder complex (HSC), driven by a musculoskeletal system has been developed in this paper, and the continuum mechanics modeling of skeletal-muscles with the evolutionary constitutive law of Hatze has been created at the same time. The constitutive equations are formulated using the link coordinates at first, and then transformed to the common global coordinate system. Based on the updated Lagrangian approach, the human multibody dynamics for a multiple bone-joints system driven by muscle activations has been formulated using the kinetic and potential energies stored in the respective muscles and bone-joint system. Since the governing equations of motion and the dynamic equilibrium equation includes statically indeterminate problems such as the multimuscles constraint for joint torques, they have been formulated, and solved, using Lagrangian multiplier approaches, under prescribed constraint and applied load conditions. Finally, an actual application to the assistive technology of a stand-up motion, aided by the humerus-shoulder complex for lifting one's own upper body, has been analysed and compared with those of experiment, and the applicability of the method developed has been clarified.

*Keywords:* humerus-shoulder complex, multimuscle activations and constraints, multibody dynamics, updated Lagrangian approach, Lagrangian multiplier's approach, muscle's statically indeterminate problems, application to assistive technology.



## 1 Introduction

Many research works aiming to clarify the dynamics of HSC system have been done extensively. Poppen and Walker [3], Dvir and Berme [4], and Engin and Peindl [5] studied the rigid link model of the shoulder complex by two or three dimensional models, and attempted to reveal the motion mechanisms of the shoulder complex in elevated motion of the upper arm. Meanwhile, van der Helm and Veenbaas [6] revealed the mechanical effect of muscles with large attachment sites for the modeling of the shoulder mechanism. In addition, Kalra et al [7] and Maurel [8] and Maurel and Thalmann [9] proposed the topological modeling based on medical data. They predicted the inner planes of the muscle forces by using the proposed shoulder complex models.

On the other hand, experimental studies have been reported by Maekawa et al [10] who measured the movements of the HSC system, using 3-D coordinates, and revealed the relationships between humerus and scapula movements in elevation, adduction, and abduction of the HSC system. Kizuka et al [11] measured the relative activation relationship of the surface and inner layers of muscles.

In most cases of the HSC system so far stated, the multibody dynamics modeling of the HSC system has been performed by using the inverse dynamics approaches. However, the assistive technology for the recoveries of diseased people require more rational approaches on the bone-muscle system of limb-trunk motions of the HSC system, since the activation levels measured at the skin surface usually differ from those of interior muscles because there exists many muscle activations at the interior of the shoulder complex.

This paper presents a more rational approach on the multi-body dynamics of the HSC system driven by the musculoskeletal system. The continuum mechanics of muscles with the evolutionary constitutive law of Hatze [1, 2] has been developed at first in order to solve the multi-muscle system stored in the shoulder complex. The Lagrange Multiplier approaches are applied to solve the statically indeterminate problems with the multimuscles constraint giving rise to joint torques. Finally, an actual application to solve a stand up motion, aided by the HSC system for lifting one's own upper body, has been analysed and compared with those of experiment. The applicability of the method developed has been clarified including rational approaches on multi-muscle activation levels.

## 2 Schematical model of humerus-shoulder complex

Fig. 1 (a) [12] shows a schematical view of the humerus-shoulder complex, which consists of 3 rigid links (a clavicle, a scapula, and a humerus) with 3 rotational joints (a sternoclavicular joint, an acromioclavicular joint, and a shoulder joint) and the scapula contacts and slide along the thorax along the scapular-thoracic joint.

Fig. 1 (b) shows the driving muscles where they generate relative movements and / or constraint between mainly the Scapula-Thorax, humerus-scapula and

humerus-Thorax and so on. The role of these muscles are shared by some parts, i.e. the muscles driving the scapula motion sliding on the thoracocis surface, muscles driving the humerus motion, and the muscles interlocking the relative motion between the humerus and scapula along the front and back surfaces, and that along the depth between the thorax and the scapula. Each muscle system constructs the antagonism system and generates various movements; i.e., elevation, reduction, abduction, adduction, and rotation of the humerus-scapula system.

In this case, referring to Fig. 1 (b), the elevating motion of the scapula consists of Trapezius (upper fibers (12)), Levator scapulae (5) and Rhomboids (6), and the reducing motion is given by the Subclavius, Pectoralis Minor (10) and Trapezius (lower fibers (12)). In the same way, the abducting motion of the Humerus is given by the Deltoid (middle fibers (13)), Supraspinatus (1), Long head of the biceps (16), and Long head of the triceps (14)), and adducting motion is given by the Pectoralis Major (3), Coracobrachialis (4), Subscapularis (2), Latissimus dorsi (7), Teres Major (9), and Short head of the biceps (15), respectively.

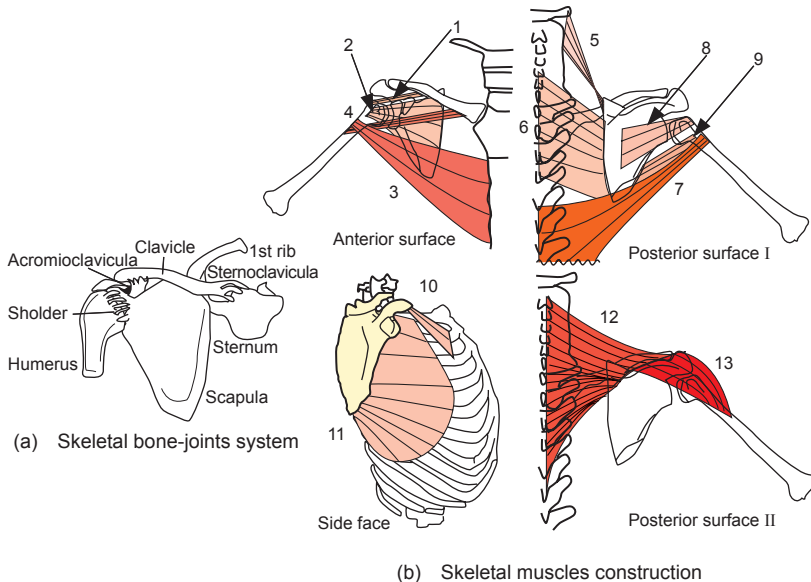


Figure 1: Schematical views of the HSC system.

### 3 Assistive motion modeling aided by the shoulder complex

Fig. 2 (a) shows a typical stand up motion of a candidate from the sitting posture during an assistive training.

The motions of the shoulder complex are shared by three steps as shown in Fig. 2 (b) i.e. adduction, abduction and elevation respectively.

Below we limited the present approaches to be the abduction / adduction motion for simplicity. Fig. 2 (c) shows the interactive forces acting on the humerus and shoulder complex, due to the driving muscle forces stated above.

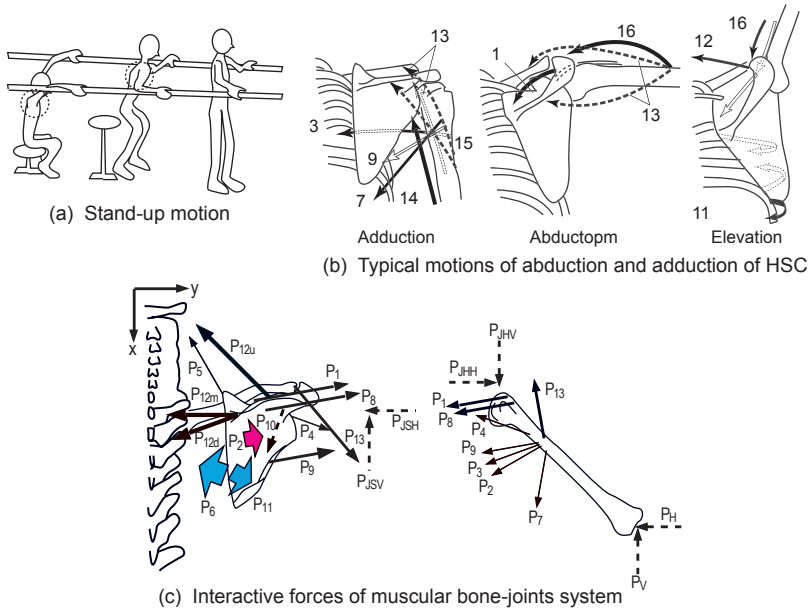


Figure 2: Assistive motion and their interactive forces of the HSC.

#### 4 Simplified modeling of the HSC

For simplicity, we assume that (1) the Humerus-shoulder complex consists of 3 rigid links (a clavicle, a scapula, a humerus), (2) the clavicle and scapula are assumed to be one rigid link because the relative motion between them is to be small during abduct and adduct motions. (3) the scapula motion is assumed to be done in 2D space (metopic plane), (4) the clavicle and scapula inertias are to be small because the clavicle moves quasi-statically during the scapula motion at the acromioclavicular joint. (5) the scapula motion at the scapular-thoracic joint is assumed to be performed by the agonists, and the viscosity between the scapula and thorax are assumed to be ignored (not to have synovial properties).

Then, the driving muscles of the shoulder complex are shared by the following five groups of muscle strips  $MS_{ij}$  ( $i$ : link number,  $j$ : muscle strip number), as shown in Fig. 3 (b). These muscle strips consists of the following five groups specified by the muscle's origin and inserted positions:

- $MS_{11}$ : Trapezius (lower fibers), Pectoralis Minor, Subclavius (Thorax clavicle-scapula muscle group),
- $MS_{12}$ : Trapezius (upper fibers), Levator scapulae, Rhomboid (Thorax clavicle-scapula muscle group),
- $MS_{21}$ : Teres Major, Coracobrachialis, Subscapularis



- (Clavicle-scapula humerus muscle group),
- $MS_{22}$ : Deltoid (middle fibers), supraspinatus
- (Clavicle-scapula humerus muscle group),
- $MS_{23}$ : Latissimus dorsi, Teres Major,
- (Thorax humerus muscle group),

where the PCSA (Physiological Cross-Sectional Area) of each muscle strip is assumed to be the sum of the grouped muscles' cross-sectional areas, and the tenoid muscles are replaced by sets of the radial line segment grouped by considering the innervation and the error of the origin/insertion position [13]. The difference of dominance between the surface and interior surface muscles are assumed to be ignored because its differences are minute.

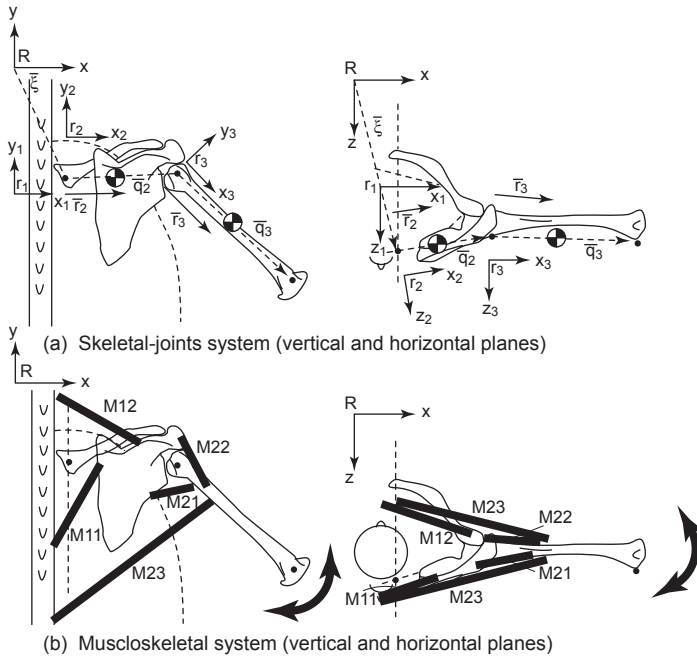


Figure 3: Computer models of the HSC coupled system.

## 5 Constitutive model of skeletal muscle

The uni-axial active stress under contraction along the muscle fibers  $S^{af}$  is expressed as follows, [2, 14] based on the evolutionary model of Hazte [1] as shown in Fig. 4 (a),

$$S^{af} = S_{max}^0 \cdot B(\beta) \cdot F(\epsilon_f) \cdot P(\dot{\epsilon}_f) \quad (1)$$

where  $S_{max}^0$  represents maximum isometric stress and  $B(\beta)$ ,  $F(\epsilon_f)$  and  $P(\dot{\epsilon}_f)$  are activation rate, force-deformation, and force-velocity relations, respectively. The



parameters  $\beta$ ,  $\varepsilon_f$ , and  $\dot{\varepsilon}_f$  represent the neuro stimulation, Green strain, and strain rate.

It can be generalized as

$$S_{xx}^{af} = D^{af}(\beta, \varepsilon_{xx}, \varepsilon_0, \dot{\varepsilon}_{xx})(\varepsilon_{xx} - \varepsilon_0) \tag{2}$$

with the following equations as

$$D^{af}(\beta, \varepsilon_{xx}, \varepsilon_0, \dot{\varepsilon}_{xx}) = D_0(\beta, \varepsilon_{xx}) \cdot B(\beta) \cdot F(\varepsilon_{xx}) \cdot G(\dot{\varepsilon}_{xx}),$$

$$B(\beta) = a_k \exp[b_k B(\beta, \varepsilon_{xx})], \quad (k = 1, 2)$$

$$F(\varepsilon_{xx}) = c_1 + c_2 \exp[R(\varepsilon_{xx}) \sin[V(\varepsilon_{xx})]], \quad G(\dot{\varepsilon}_{xx}) = \left[ \frac{(G_0 + a)b}{\dot{\varepsilon}_{xx} + b} - a \right] / G_0,$$

$$R(\varepsilon_{xx}) = -\mu_1 \varepsilon_{xx}, \quad V(\varepsilon_{xx}) = \mu_2(\varepsilon_{xx} + c_3)$$

where  $F(\varepsilon_{xx})$  represents the normalized function of force-deformation relations,  $D_0(\beta, \varepsilon_{xx})$  the parameter for the transformation to the global coordinate. The relationship between stress and strain on the global coordinate is given by multiplying  $F(\varepsilon_{xx})$  by  $D_0(\beta, \varepsilon_{xx})$ . The parameters  $a_{bk}$ ,  $b_{bk}$  ( $k = 1, 2$ ),  $a_m$ ,  $b_m$ ,  $c_i$  ( $i = 1, 2, 3$ ),  $G_0$ , and  $\mu_i$  ( $i = 1, 2$ ) are the material factors and  $\varepsilon_{xx}$  means the strain from the initial length. In this paper,  $B(\beta)$  is replaced approximately by  $\beta$  for simplicity.

In addition,  $D^{af}$  expresses a function of neuro stimulation  $\beta$  defining the muscle force under isotropic condition, and  $\varepsilon$  and  $\phi$  ( $=\varepsilon - \varepsilon_0$ ) are independent parameters. The neuro stimulation  $\beta$  must be provided to satisfy the strain required to generate movements  $\varepsilon$  and the muscle contraction force  $\sigma = D^{af}\phi$ , which counteract with the external force, to satisfying the dynamic equilibrium condition.

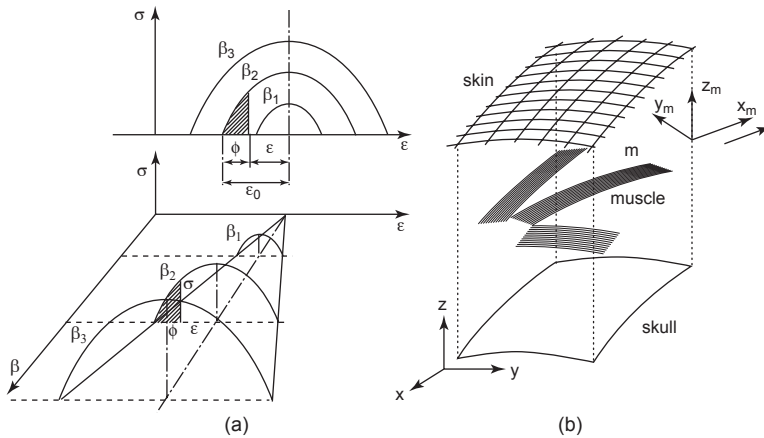


Figure 4: The stimulation and contraction-deformation characteristics of a muscle.

Using the above equations, we can obtain the incremental form of constitutive equation for skeletal muscle as below. Since the active type constitutive equation shown in Eq. (2) is the function of  $\beta$ ,  $\varepsilon_{xx}$ ,  $\varepsilon_0$ , and  $\dot{\varepsilon}_{xx}$ , the incremental form of constitutive equation on  $n$ -th step can be expressed as follows

$$\begin{aligned} \Delta S_{xx}^{af} &= \Delta D^{af} \{(\varepsilon_{xx}^{n-1} + \Delta \varepsilon_{xx}^n) - (\varepsilon_o^{n-1} + \Delta \varepsilon_o^n)\} + D^{af} (\Delta \varepsilon_{xx}^n - \Delta \varepsilon_o^n) \\ \Delta D^{af} &= \frac{\partial D^{af}}{\partial \beta} \Delta \beta^n + \frac{\partial D^{af}}{\partial \varepsilon_{xx}} \Delta \varepsilon_{xx}^n + \frac{\partial D^{af}}{\partial \dot{\varepsilon}_{xx}} \Delta \dot{\varepsilon}_{xx}^n \end{aligned} \quad (3)$$

### 6 Musculoskeletal modeling of the HSC system

Fig. 3 (a) shows a computer model of the HSC system with 2 rigid links and 2 rotational joints, surrounded by several driving muscles groups. The 1st link consists of clavicle and scapula and the 2nd link defines the Humerus. Fig. 3 (a) shows the coordinate systems of  $r_1, r_2,$  and  $r_3,$  representing the partial coordinates of the thorax, those of the 1st and 2nd links,  $R$  being the global coordinate respectively. The position vectors among partial coordinates are expressed by  $\bar{r}_i, \bar{q}_i, \xi_i$  and so on, in vertical and horizontal planes. Then, the positional vector at the center of gravity of  $i$ -th link  $\{\bar{r}_{i+1}\}^R$  and the velocity vector at center of gravity,  $\{v_{i+1}\}$  can be written in the following forms

$$\begin{aligned} \{\bar{r}_{i+1}\}^R &= \{\bar{\xi}\}^T + \sum_{i=2}^i \{\bar{q}_i\}^{r_i T} [S^{i,0}] + \{\bar{r}_{i+1}\}^{r_{i+1} T} [S^{i+1,0}] \\ \{v_2\}^T &= \frac{d}{dt} \{\bar{r}_{i+1}\}^R = \{\dot{\bar{\xi}}\}^T + \sum_{i=2}^i \{\dot{\bar{q}}_i\}^{r_i T} [S^{i,0}] + \{\dot{\bar{r}}_{i+1}\}^{r_{i+1} T} [S^{i+1,0}] \end{aligned} \quad (4)$$

where

$$[S^{i,0}] = [S^{i,i-1}] [S^{i-1,i-2}] \dots [S^{2,0}] \quad (5)$$

where  $[S]^{i, i-1}$  means the coordinates transformation matrix between  $i$  and  $i-1$  members.

The translational velocity increments at the center of gravities of the 1st and 2nd links can be expressed as follows:

$$\begin{aligned} \{\Delta v_2\}^T &= \begin{bmatrix} \frac{\partial v_{2x}}{\partial \xi_x} & \frac{\partial v_{2x}}{\partial \xi_y} & \frac{\partial v_{2x}}{\partial \gamma_1} & \frac{\partial v_{2x}}{\partial \dot{\gamma}_1} \\ \frac{\partial v_{2y}}{\partial \xi_x} & \frac{\partial v_{2y}}{\partial \xi_y} & \frac{\partial v_{2y}}{\partial \gamma_1} & \frac{\partial v_{2y}}{\partial \dot{\gamma}_1} \\ 0 & 0 & 0 & 0 \end{bmatrix} \begin{Bmatrix} \Delta \xi_x \\ \Delta \xi_y \\ \Delta \gamma_1 \\ \Delta \dot{\gamma}_1 \end{Bmatrix} \\ \{\Delta v_3\}^T &= \begin{bmatrix} \frac{\partial v_{3x}}{\partial \xi_x} & \frac{\partial v_{3x}}{\partial \xi_y} & \frac{\partial v_{3x}}{\partial \gamma_1} & \frac{\partial v_{3x}}{\partial \dot{\gamma}_1} & \frac{\partial v_{3x}}{\partial \gamma_2} & \frac{\partial v_{3x}}{\partial \dot{\gamma}_2} \\ \frac{\partial v_{3y}}{\partial \xi_x} & \frac{\partial v_{3y}}{\partial \xi_y} & \frac{\partial v_{3y}}{\partial \gamma_1} & \frac{\partial v_{3y}}{\partial \dot{\gamma}_1} & \frac{\partial v_{3y}}{\partial \gamma_2} & \frac{\partial v_{3y}}{\partial \dot{\gamma}_2} \\ 0 & 0 & 0 & 0 & 0 & 0 \end{bmatrix} \begin{Bmatrix} \Delta \xi_x \\ \Delta \xi_y \\ \Delta \gamma_1 \\ \Delta \dot{\gamma}_1 \\ \Delta \gamma_2 \\ \Delta \dot{\gamma}_2 \end{Bmatrix} \end{aligned} \quad (6)$$

Thus, the partial angular velocity  $\dot{q}_i$ , the increment of partial angular velocity  $\Delta \dot{q}_i$ , the global angular velocity  $\omega_i$ , can be obtained in the same way as above.

In the next place, the length vectors of each muscle strip of  $MS_{ij}, \{MS_{ij}^O\}^{rk}$  and  $\{MS_{ij}^I\}^{rk}$  shown in Fig. 3 (b) can be derived using the above equations.

That is, the origin of position vector,  $\{MS^O\}^R$ , positional vector  $\{MS^I\}^R$  and position vector to the 2nd link  $\{MS^I_2\}^R$  of muscle strip  $MS_{ij}$  can be expressed by

$$\begin{aligned} \{MS^O\}^R &= \{\bar{\xi}_1\}^T + \{MS^O\}r_1^T[S^{10}] \\ \{MS^{I_1}\}^R &= \{\bar{\xi}\}^T + \{MS^{I_1}\}r_2^T[S^{20}] \\ \{MS^{I_2}\}^R &= \{\bar{\xi}\}^T + \{\bar{q}_2\}r_2^T[S^{20}] + \{MS^{I_2}\}r_3^T[S^{30}] \end{aligned} \tag{7}$$

from which we have

$$MS_{l_{ij}} = \|\{MS_{ij}^I\}^R - \{MS_{ij}^O\}^R\|$$

Then we can get the strain, strain increment and strain rate increment as

$$\varepsilon_{xx}^{ij} = \frac{MS_{l_{ij}} - L_o^{ij}}{L_o^{ij}}, \quad \Delta\varepsilon_{xx}^{ij} = \sum_{k=1}^2 \frac{\partial\varepsilon_{xx}^{ij}}{\partial q_k} \Delta q_k \tag{8}$$

and

$$\Delta\dot{\varepsilon}_{xx}^{ij} = \sum_{k=1}^2 \frac{\partial\varepsilon_{xx}^{ij}}{\partial q_k} \Delta\dot{q}_k + \sum_{k=1}^2 \frac{\partial\varepsilon_{xx}^{ij}}{\partial \dot{q}_k} \Delta\dot{q}_k \tag{9}$$

## 7 Musculoskeletal system modeling based on updated Lagrangian approach

Multi-body dynamics of the HSC system consists of various nonlinearities such as angular motion of each link, the transformation matrix and their derivatives of link coordinates, the contraction dynamics of skeletal muscles due to the neuro stimulations and so on.

So we have to formulate such problems, based on the Updated Lagrangian approaches by defining numerous energies in every incremental step of motion and loading. The Updated Lagrangian Approach for solving the above problems can be expressed by

$$\frac{d}{dt} \left[ \frac{\partial\Delta L}{\partial\Delta\dot{q}_k} \right] - \frac{\partial\Delta L}{\partial\Delta q_k} = -\Delta Q_{exk} \quad (k = 1, 2, \dots) \tag{10}$$

where  $\Delta L = \Delta T - \Delta U$ , and  $\Delta T$  is the incremental kinetic energies of the whole system, by assembling those energy  $\Delta T_i$  of  $i$ -th link being expressed by translational and rotational components as,

$$\Delta T = \sum \Delta T_i = \sum \frac{1}{2} \{\Delta v_i\}^T [M_i] \{\Delta v_i\} + \frac{1}{2} \{\Delta \omega_i\}^T [I_i] \{\Delta \omega_i\} \tag{11}$$

in the above  $[M_i]$  and  $[I_i]$  are mass and inertia matrices.

In the same way the incremental potential energy of the whole system and the  $i$ -th muscle strip  $\Delta U_{mij}$ , of the muscle MS<sub>ij</sub>, the incremental potential energy of the whole system  $\Delta U$  can be expressed by

$$\Delta U = \sum_{i,j} \Delta U_{m_{ij}} = \sum_{i,j} \frac{1}{2} PCSA_{i,j} L_o^{ij} \Delta\phi_{xx}^{ij} \Delta S_{xx}^{\alpha_f ij} \tag{12}$$

where  $\Delta S_{xx}^{\alpha_f ij}$  is the incremental active stress in a muscle, and  $\Delta\phi_{xx}^{ij} = \Delta\varepsilon_{xx} - \Delta\varepsilon_o$  means the constraint strain of muscle contraction,  $L_{oij}$  and  $PCSA_{ij}$  being the



natural length of muscle and the physiological cross-sectional area, respectively. Note that the component of passive stress is neglected for simplicity. Then Eq. (10) can be rewritten for the  $k$ -th link as follows

$$\frac{d}{dt} \left[ \frac{\partial \Delta T}{\partial \Delta \dot{q}_k} \right] - \frac{\partial \Delta T}{\partial \Delta q_k} - \sum \left[ \frac{d}{dt} \left\{ \frac{\partial \Delta U_{m_{ij}}}{\partial \Delta \dot{q}_k} \right\} - \frac{\partial \Delta U_{m_{ij}}}{\partial \Delta q_k} \right] = -\Delta Q_{ex_k} \quad (13)$$

and the left hand terms of Eq. (13) can be further expanded as follows, by neglecting the second order term, that is

$$\begin{aligned} & \frac{d}{dt} \left[ \frac{\partial \Delta T}{\partial \Delta \dot{q}_k} \right] - \frac{\partial \Delta T}{\partial \Delta q_k} - \sum \left[ \frac{d}{dt} \left\{ \frac{\partial \Delta U_{m_{ij}}}{\partial \Delta \dot{q}_k} \right\} - \frac{\partial \Delta U_{m_{ij}}}{\partial \Delta q_k} \right] \\ &= \frac{d}{dt} \left[ \frac{\partial \Delta T}{\partial \Delta \dot{q}_k} \right] - \frac{\partial \Delta T}{\partial \Delta q_k} - \sum \left[ \frac{d}{dt} \left\{ \frac{\partial \Delta U_{m_{ij}}}{\partial \Delta \dot{\varepsilon}_{xx}^{ij}} \frac{\partial \Delta \varepsilon_{xx}^{ij}}{\partial \Delta \dot{q}_k} \right\} \right. \\ & \quad \left. - \frac{\partial \Delta U_{m_{ij}}}{\partial \Delta \dot{\varepsilon}_{xx}^{ij}} \frac{\partial \Delta \varepsilon_{xx}^{ij}}{\partial \Delta q_k} - \frac{\partial \Delta U_{m_{ij}}}{\partial \Delta \varepsilon_{xx}^{ij}} \frac{\partial \Delta \varepsilon_{xx}^{ij}}{\partial \Delta q_k} \right] \end{aligned} \quad (14)$$

### 8 Dynamic equations of motion for whole system

The dynamic equations of motion for the whole system can be expressed as

$$\begin{aligned} [M] \{ \Delta \ddot{q} \} + [C] \{ \Delta \dot{q} \} + [K] \{ \Delta q \} + [A_1] \{ \Delta q \} + [A_2] \begin{Bmatrix} \Delta q \\ \Delta \dot{q} \end{Bmatrix} \\ = - \{ \Delta Q_{ex} \} - [B_1] \{ \Delta q \} - [B_2] \{ \Delta \phi^{ij} \} \end{aligned} \quad (15)$$

where  $[A_1]$  and  $[A_2]$  are the terms of muscle stiffness and viscosity, and 2nd and 3rd terms of the right side are the muscle force for motion generation, muscle inner force for dynamic torque balance at respective joints, respectively. It has been postulated that the incremental joint torques generated in the 1st term of the right side in Eq. (15) should be balanced with the incremental muscle torques of the 3rd term. That is, the dynamic equilibrium equation at each joint is expressed by

$$- \{ \Delta Q_{ex} \} - [B_2] \{ \Delta \phi^{ij} \} = 0 \quad (16)$$

where Eq. (16) includes a statically indeterminate problem in case where there are many muscle strips acting on a joint. If Eqs. (16) satisfy, then Eqs. (15) can be rewritten by

$$[M] \{ \Delta \ddot{q} \} + [C] \{ \Delta \dot{q} \} + [K] \{ \Delta q \} + [A_1] \{ \Delta q \} + [A_2] \begin{Bmatrix} \Delta q \\ \Delta \dot{q} \end{Bmatrix} = - [B_1] \{ \Delta q \} \quad (17)$$

### 9 Dynamic equilibrium equation using the Lagrange multipliers approach

In parallel with motion analysis given by Eq. (17), we consider the yielding conditions of the incremental muscle contraction forces based on Eq. (16). The equilibrium equation between external and internal forces in the model with 2 rigid links and 5 muscles shown in Fig. 3 (a) can be expressed as follows,



$$\begin{aligned}
 \mathbf{F}_{11} + \mathbf{F}_{12} - \mathbf{F}_{21} - \mathbf{F}_{22} + \mathbf{R}_1 - \mathbf{R}_2 + \mathbf{G}_1 &= 0, \\
 \mathbf{F}_{21} + \mathbf{F}_{22} - \mathbf{F}_{23} + \mathbf{R}_2 + \mathbf{G}_1 + \mathbf{F}_{ex} &= 0, \\
 \mathbf{T}_{11}(\mathbf{F}_{11}) + \mathbf{T}_{12}(\mathbf{F}_{12}) - \mathbf{T}'_{21}(\mathbf{F}_{21}) - \mathbf{T}'_{22}(\mathbf{F}_{22}) + \mathbf{T}_{R2}(\mathbf{R}_2) + \mathbf{T}_{G1}(\mathbf{G}_1) &= 0, \\
 \mathbf{T}_{21}(\mathbf{F}_{21}) + \mathbf{T}_{22}(\mathbf{F}_{22}) + \mathbf{T}_{23}(\mathbf{F}_{23}) + \mathbf{T}_{G2}(\mathbf{G}_2) + \mathbf{T}_{ex}(\mathbf{G}_{ex}) &= 0
 \end{aligned} \tag{18}$$

where  $\mathbf{F}_{ij}$ ,  $\mathbf{R}_i$ ,  $\mathbf{G}_i$ , and  $\mathbf{F}_{ex}$  represent the muscle force, the joint reaction force, gravity force, and external force vector respectively,  $\mathbf{T}(\mathbf{X})$  being the moment due to the force  $\mathbf{X}$  about the origin of each partial coordinate. In addition to the above,  $\mathbf{X}_i$  ( $i = 1, 2, \dots, 5$ ) are the generated forces of muscle strip  $\{\mathbf{X}_i\}^T = \{\mathbf{F}_{11}, \mathbf{F}_{12}, \mathbf{F}_{21}, \mathbf{F}_{22}, \mathbf{F}_{23}\}$  and  $\mathbf{X}_i$  ( $i = 6, 7, \dots, 9$ ) being the reaction force acting on each joint.

Since the governing equilibrium equations, obtained from Eqs. (18) generally include much more numbers of unknowns than those of equilibrium equations at each joints, since they include a lot of unknown forces of muscle strips as shown in Fig. 3.

In order to solve the problem, we apply the Lagrangian multiplier's approach as shown below. Let us introduce a Lagrangian function as

$$L(\mathbf{X}, \lambda) = f(\mathbf{X}) - \sum \lambda_i h_i \tag{19}$$

where  $f(\mathbf{X})$  is given by

$$f(\mathbf{X}) = \sum_{i=1}^5 C_i (\mathbf{X}_i)^2 + \sum_{i=1}^4 (\mathbf{X}_{5+i})^2 \tag{20}$$

and  $\lambda_i$  the Lagrangian multipliers,  $h_i$  being the constraint conditions given in Eqs. (18),  $C_i$  the weight parameters which indicate the rating of muscle force to these problems, respectively.

Then the Lagrangian function given in Eq (19) must satisfy the extremity's conditions with respect to the joint forces  $\mathbf{X}_i$  and Lagrange parameter  $\lambda_i$  as follows.

$$\frac{\partial L(\mathbf{X}, \lambda)}{\partial \mathbf{X}_i} = 0 \quad (i = 1, \dots, 9) \quad , \quad \frac{\partial L(\mathbf{X}, \lambda)}{\partial \lambda_i} = 0 \quad (i = 1, \dots, 6) \tag{21}$$

Once we can get the minimum conditions of muscle forces to satisfy Eq. (19), by solving Eq. (21), then we can get the muscle activation levels directly using the rational approach stated above as follows.

$$\beta_{ij} = \left| \frac{D_{ij}^{af(-\beta)} \varepsilon_{xx}^{ij} - \sqrt{(D_{ij}^{af(-\beta)} \varepsilon_{xx}^{ij})^2 + 4 \cdot D_{ij}^{af(-\beta)} S_{xx}^{afij}}}{2 \cdot D_{ij}^{af(-\beta)}} \right| \tag{22}$$

where  $D_{ij}^{af(-\beta)} = D_{ij}^{af} / \beta^{ij}$ . At the same time, the torques generated by joint reaction, gravity and external forces can be computed on every step of posture during movements.



## 10 Analysis and experiments on stand-up motion assisted by the HSC system

The movement of the HSC system during lifting one's upper trunk, using both elbows, as shown in Fig. 3 (a) and Fig. 5 is analysed and the results are compared with those obtained by experiments.

A volunteer aged 23 weighing 60 kgf was examined to measure the humerus postures of the shoulder angles with 90, 70, and 50 [deg.] during 2 seconds, under with or without loading conditions of 10kgf, respectively.

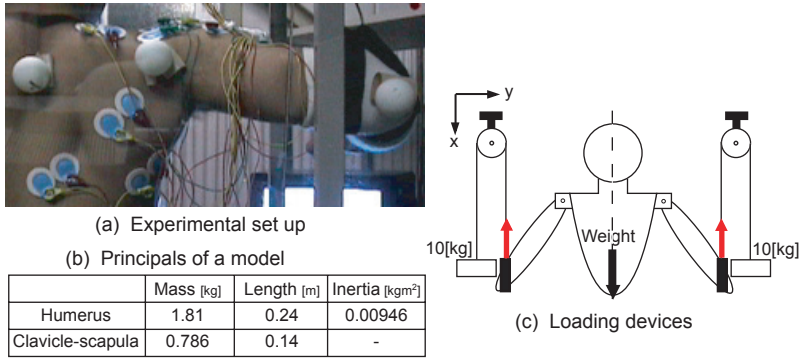


Figure 5: Experiments on stand-up motion and EMG measurements.

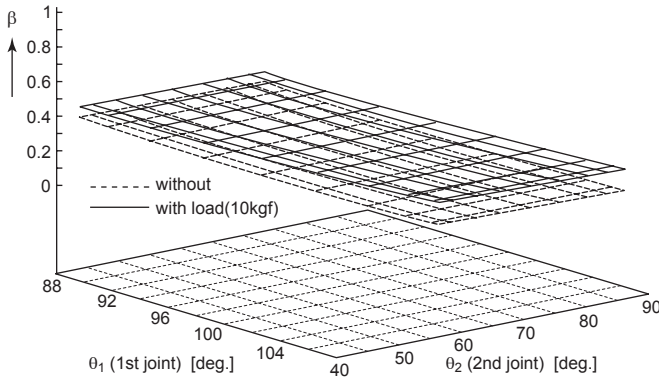


Figure 6: Computed activation levels of MS11.

A video camera was used to measure the posture during the movements, and EMG data of every muscles such as MS<sub>11</sub>, MS<sub>12</sub>, MS<sub>21</sub>, MS<sub>22</sub>, MS<sub>23</sub> were recorded as, shown in Fig. 5 (a)

Fig.6 shows an example of the computed activation levels  $\beta$  of muscle strip, MS<sub>11</sub>, during angle changes in every step of the HSC motions, with or without additional load conditions of 10kgf. It is seen that the muscle activation level increases with both the joint angle and the amount of load level, respectively.

Fig. 7 (a) shows the difference in the calculated activation levels of the agonist muscle  $MS_{11}$  (Trapezius lower fibers) and antagonist muscle  $MS_{12}$  (Trapezius upper fibers) during the angle change at  $i$ -th joint in the posture from (a-1) ( $\theta_1 = 112$  (deg.),  $\theta_2 = 65$ ), to (a-3) ( $\theta_1 = 86$ ,  $\theta_2 = 33$ ), respectively. It is seen that the activation level of the muscle  $MS_{11}$  is more greatly increased than that of  $MS_{12}$ , and the agonist M. (muscle) gives rise to main force generator, counteracting to given loads.

Fig. 7 (b) ~ (d) show the comparison between the measured and calculated results levels of  $MS_{21}$  and  $MS_{23}$ , during the increase of humerus adductive motions. The computed activation levels of each muscle satisfactorily agree well with those of the experimental, except that the activation levels of  $MS_{23}$  during the lower angular motion, which seem to include the shearing effect were omitted for simplicity.

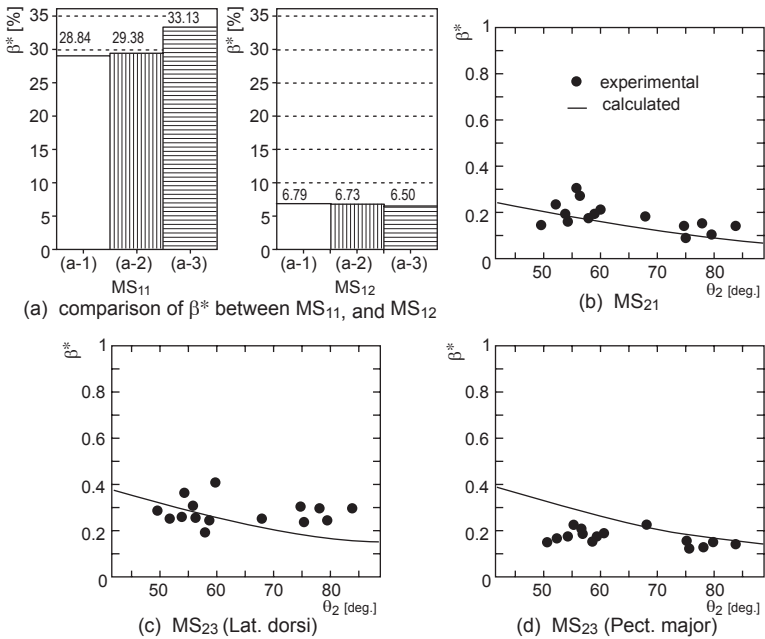


Figure 7: Comparison of EMG between calculated and measured.

In the next, an experiment on the adduct motions of a volunteer's elbows, using the belt-pulley system as shown in Fig. 5 (c) have been done, accompanied with lifting additional force 10kgf in each belt load at the same time, whereas the adductive motion take places one second from the respective horizontal planes. The computer analysis has been done at the same time with the sampling time of  $10^{-5}$  sec.

Fig. 8 (a) (b) and (c) shows the comparison between calculated and measured results with respect to the joint angular motion (Fig. (a)), joint angles (Fig. (b)) and angular velocities (Fig. (c)) during the time history of motions. It is seen that the computed results during motion trajectories agree well with those of the experimental, and the relation between joint torques and angles satisfactorily be calculated without any measurements and without any inverse dynamic approaches.

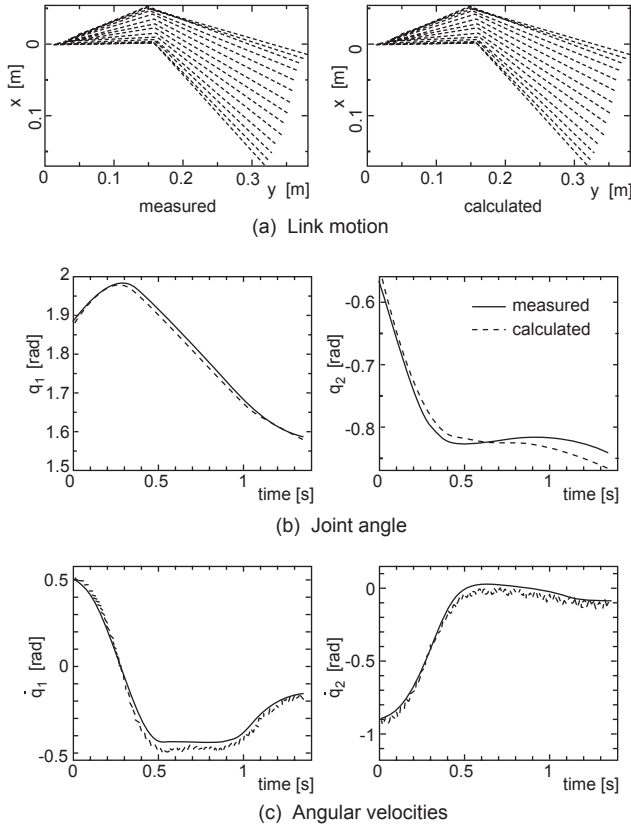


Figure 8: Comparison of link motion, joint angles and angular velocities.

## 11 Concluding remarks

The following results are obtained.

- (1) The continuum mechanics modeling of multimuscule systems with evolutionary constitutive law has been developed for solving the multi-musculoskeletal system such as humerus-shoulder complex.
- (2) The humerus-clavicle-scapula-thorax system with three rigid links, driven by numerous multimuscule system has been formulated and applied to the humerus-shoulder complex for lifting one's upper body. It is made clear



that the present approach can successfully be applied to these kinds of problems.

- (3) The Updated Lagrange approach and the Lagrange Multiplier approach can successfully be applied to solve the statically indeterminate problems with multimuscles constraint, larger than the number of governing dynamic equilibrium equations at each joint, and on each loading step.
- (4) Once this kind of approach has been developed, it makes possible that one can calculate numerous kinds of activation levels of multi-muscle system rationally, without any measurements under inverse approaches.

## References

- [1] H. Hatze, A myocybernetic control model of skeletal muscle, *Biological Cybernetics*, Vol. 25, pp. 103-119, 1977.
- [2] T. Tsuta, et al, Muscle's continuum mechanics and FEM simulation on facial expression for muscle ~ soft tissue combined system, *Bulletin of the Faculty of Engineering, Hiroshima University*, Vol. 46, pp. 59-71, 1997. (In Japanese)
- [3] N. K. Poppen & P. S. Walker, Forces at the glenohumerul joint in abduction, *Clin. Orthop. Rel. Res*, Vol. 135, pp. 165-170, 1978.
- [4] Z. Dvir & N. Berme, The shoulder complex in elevation of the arm, A mechanism approach, *Journal of Biomechanics*, Vol. 11, pp. 219-225, 1978.
- [5] A. E. Engin & R. D. Peindl, On the biomechanics of human shoulder complex -I. Kinematics for Determination of the shoulder complex sinus, *Journal of Biomechanics*, Vol. 20, pp. 103-117, 1987.
- [6] F. C. T. van der Helm & R. Veenbaas, Modeling the mechanical effect of muscles with large attachment sites: Application to the shoulder mechanism, *Journal of Biomechanics*, Vol. 24, pp. 1151-1163, 1991.
- [7] P. Kalra, et al, Topological modeling of human anatomy using medical data, in *Proceedings of the Computer Animation '95*, pp. 172-180, 1995.
- [8] W. Maurel, 3D modeling of the human upper limb including the biomechanics of joints, muscles and soft tissues, Ph. D. Thesis 1996, *Laboratoire d'Infographie-Ecole Polytechnique Federale de Lavusanne*, 1999.
- [9] W. Maurel & D. Thalmann, A case study on human upper limb modeling for dynamic simulation, *Computer Methods in Biomechanics and Biomedical Engineering*, Vol. 2, pp. 1-17, 1999.
- [10] K. Maekawa, et al, Motion analysis of the shoulder complex, *Biomechanism*, Vol. 11, pp. 133-141, 1992. (In Japanese)
- [11] T. Kizuka, et al, Electromyographic Analysis of shoulder muscles to determine effective ranges for loads and motion during low-level shoulder exercises, *Biomechanism*, Vol. 15, pp. 214-223. (In Japanese)
- [12] V. M. Zatsiorsky, Kinematics of human motion, *Human Kinetics*, 1999.



- [13] G. R. Johnson, D. Spalding, et al, Modeling the muscles of the scapula morphometric and coordinate data and functional implications, *Journal of Biomechanics*, Vol. 29, pp. 1039-1051, 1996.
- [14] T. Tsuta, et al, Continuum mechanics of facial muscle and creep relaxation remodeling analysis of muscle-skin system, *Computer Methods in Biomechanics & Biomedical Engineering*, Vol. 3, pp.199-206, 2001.

